Hindawi Publishing Corporation
Mathematical Problems in Engineering
Volume 2015, Article ID 716352, 9 pages
http://dx.doi.org/10.1155/2015/716352

Research Article

The Two-Dimensional Heat Transfer Analysis in Arrayed Fins with the Thermal Dissipation Substrate

Hai-Ping Hu

Department of Marine Engineering, National Taiwan Ocean University, Keelung 20224, Taiwan

Correspondence should be addressed to Hai-Ping Hu; hphu@ntou.edu.tw

Received 10 July 2014; Revised 20 October 2014; Accepted 22 October 2014

Academic Editor: Hua Fan

The aim of the present study is to investigate the two-dimensional heat transfer analysis in arrayed fins with thermal dissipation substrate. The governing equations for the fins and the substrate are expressed with Laplace equations, and the boundary conditions around the fins and substrate are Robin conditions. The present investigation first aims to provide a solution with regard to the geometry models by a series truncation method. Then the research will compare the results of the series truncation method with the point-matching method. Furthermore, the present study will also discuss the effects of dimension and Biot number of the fins on local dimensionless temperature, mean temperature, and heat transfer rate.

1. Introduction

Fins are used mainly to increase the extent of the heat transfer surface area in order to enhance the overall heat transfer or heat flux. The application of the fins and the thermal substrate widely ranges with regard to the larger scale and small scale of the heat cooling, power plant, chemical reactors, air condition equipment, and many other units where thermal heat is generated and must be transferred from high temperature to low temperature. Some important researches in the early stages have been based on one-dimensional or two-dimensional, steady state analysis. For example, Levitsky [1] investigated the criteria for validity of the one-dimensional fin approximation. The analysis of temperature distribution and heat flux in fins customarily makes use of a one-dimensional fin approximation. Irey [2] compared the errors between the one-dimensional and two-dimensional fin solutions, and the ratios of the interior to exterior resistance and the Biot number. The results showed that only for a small Biot number is the one-dimensional solution a satisfactory approximation. Lau and Tan [3] investigated the errors in one-dimensional heat transfer analysis in straight and annular fins. Compare one-dimensional analysis with two-dimensional analysis. The presented error decreases with decreasing values of thermal conductivity. Sparrow and Lee [4] researched the effects of fin base-temperature depression in a multifin array.

In the present approach, the temperature in the tube wall was determined via a solution of Laplace's equation. Suryanarayana [5] analyzed the two-dimensional effects on heat transfer rates from an array of straight fins and examined the errors involved in computing the heat transfer rates from fins on the basis of uniform base temperature. Heggs and Stones [6] investigated the effects of dimensions on the heat flow rate through extended surfaces, comparing one- and two-dimensional heat flows through longitudinal and annular fin assemblies for a wide range of system parameters. Heggs et al. [7] investigated the two-dimensional analysis of fin assembly heat transfer by a series truncation method. They showed that the series truncation method yields accurate solutions even for problems for which the finite-difference and finite-element methods fail to provide acceptable results.

Manzoor et al. [8] researched the accuracy of perfect contact fin assembly analysis. Their work can easily be extended to annular geometry and to include fins with tapered or curved fin profile. Recently, Wood et al. [9] researched the performance indicators for steady-state heat transfer through fin assemblies; they presented several models describing steady-state heat flow through an assembly consisting of a primary wall and attached extended fin. For transient analysis of heat conduction, Wang et al. [10] established a new computing method for the cubic spline difference method for the heat conduction problem. Next, Wang et al. [11]

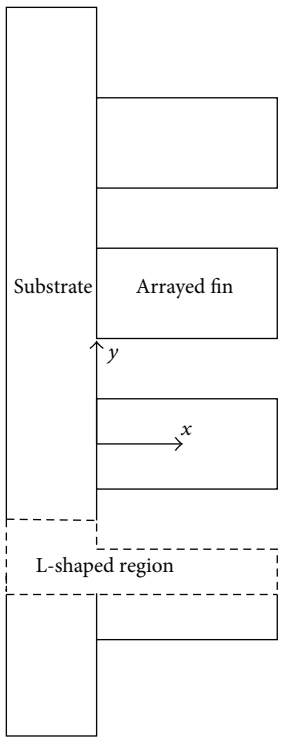

Figure 1: Physical model and coordinate system.

developed a highly accurate numerical method named the cubic spline difference method and investigated the transient heat conduction problems. Mabood et al. [12] researched the series solution for steady heat transfer in a heat-generating fin and applied the optimal homotopy asymptotic method for the approximate solution of steady state of heat-generating fin with simultaneous surface convection and radiation.

Since the fins are widely applied in thermal and energy engineering, the aim of the present study is to investigate the two-dimensional heat transfer analysis in arrayed fins with thermal dissipation substrate. First, the present investigation focuses on the substrate and fin by a series truncation method. Next, the research compares the results from the series truncation method with the point-matching method and compares the precision by using both methods. Furthermore, the study also discusses in detail the different parameters, for example, dimension of the fins and substrate, Biot number on the local dimensionless temperature, mean temperature, and heat transfer rate.

2. Analysis

Consideration of the heat transfer of thermal dissipation substrate and arrayed fins is under the assumption of steady state, constant thermal conductivities, uniform heat transfer coefficients, and perfect thermal dissipation of substrate-to-fin contact. The physical model is shown in Figure 1. The geometrical symmetry of an assembly of equally spaced longitudinal rectangular fins attached to a thermal dissipation substrate indicates that it is only necessary to examine that direction of the thermal dissipation substrate and fin, shown schematically in Figure 2. The governing equation for temperature distribution in the thermal dissipation substrate can be expressed as

$$\nabla^2 T_1(x, y) = 0. \tag{1}$$

And the boundary conditions of (1) are

$$\begin{aligned} \frac{\partial T_1}{\partial y} &= 0, \quad y = p, \quad -w \le x \le 0, \\ \frac{\partial T_1}{\partial y} &= 0, \quad y = 0, \quad -w \le x \le 0, \\ -k_1 \frac{\partial T_1}{\partial x} &= h_{\infty 1}(T - T_{\infty 1}), \quad -x = w, \quad 0 \le y \le p. \end{aligned} \tag{2}$$

The governing equation for temperature distribution in the fin can be expressed as

$$\nabla^2 T_2(x, y) = 0. \tag{3}$$

And the boundary conditions of (3) are

$$\begin{aligned} -k_2 \frac{\partial T_2}{\partial y} &= h_{\infty 2}(T_2 - T_{\infty 2}), \quad y = t, \quad 0 \le x \le l, \\ \frac{\partial T_2}{\partial y} &= 0, \quad y = 0, \quad 0 \le x \le l, \\ -k_2 \frac{\partial T_2}{\partial x} &= h_{\infty 2}(T_2 - T_{\infty 2}), \quad x = l, \quad 0 \le y \le t. \end{aligned} \tag{4}$$

The following dimensionless variables and equations are now defined:

$$\begin{aligned} X &= \frac{x}{p}, \qquad Y = \frac{y}{p}, \qquad \theta_1 = \frac{T_1(x, y) - T_{\infty 2}}{T_{\infty 1} - T_{\infty 2}}, \\ \theta_2 &= \frac{T_2(x, y) - T_{\infty 2}}{T_{\infty 1} - T_{\infty 2}}, \\ L &= \frac{l}{p}, \qquad W = \frac{w}{p}, \qquad T = \frac{t}{p}, \qquad k = \frac{k_2}{k_1}, \\ \mathrm{Bi}_1 &= \frac{h_{\infty 1} p}{k_1}, \qquad \mathrm{Bi}_2 = \frac{h_{\infty 2} p}{k_1}. \end{aligned} \tag{5}$$

Furthermore, the governing equations and the boundary conditions of the thermal dissipation substrate can be rewritten as dimensionless equations in the following form:

$$\nabla^2 \theta_1(X, Y) = 0, \tag{6}$$

$$\begin{aligned} \frac{\partial \theta_1}{\partial Y} &= 0, \quad Y = 1, \quad -W \le X \le 0, \\ \frac{\partial \theta_1}{\partial Y} &= 0, \quad Y = 0, \quad -W \le X \le 0, \\ \frac{\partial \theta_1}{\partial X} &= -\mathrm{Bi}_1(1 - \theta_1), \quad X = -W, \quad 0 \le Y \le 1. \end{aligned} \tag{7}$$

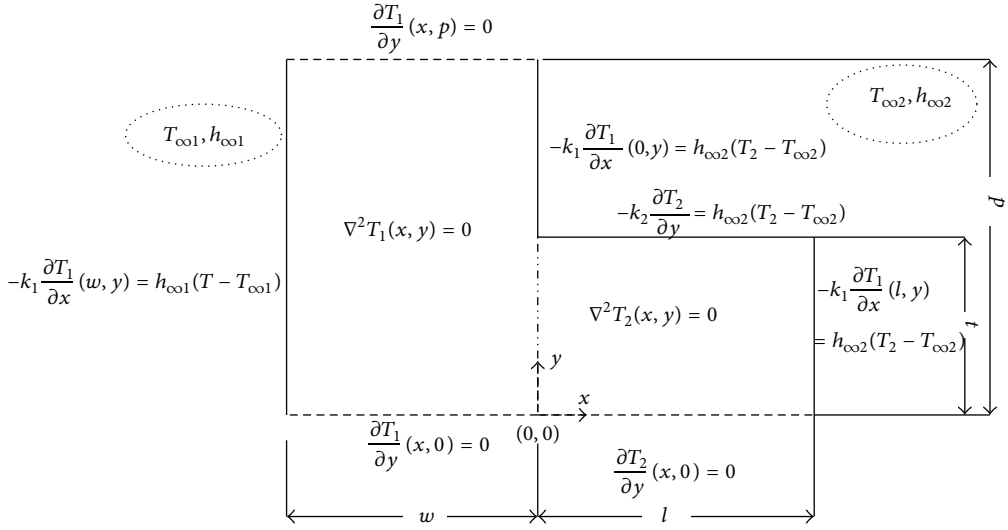

Figure 2: The L-shaped regions and boundary conditions.

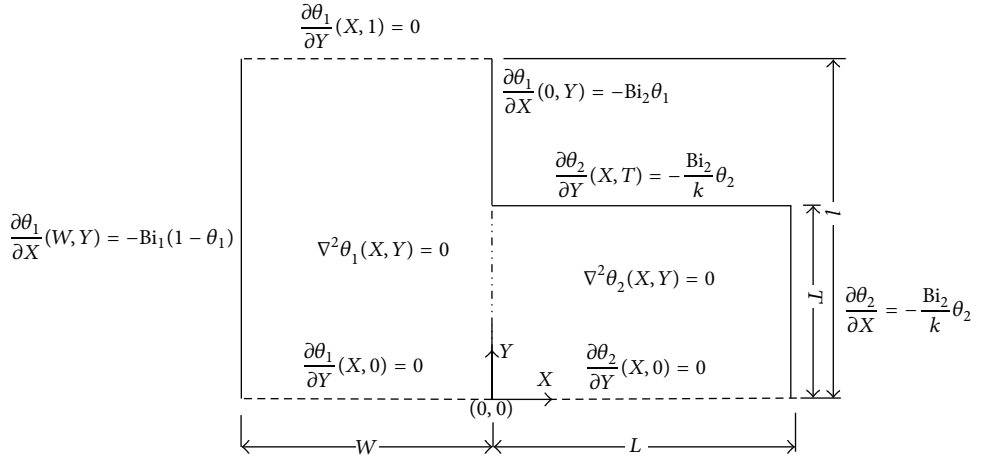

Figure 3: The L-shaped regions with the dimensionless governing equations and the boundary conditions.

The governing dimensionless equation (Figure 3) for the fin is

$$\nabla^2\theta_2(X,Y)=0, \tag{8}$$

$$\frac{\partial \theta_2}{\partial Y}=-\frac{\mathrm{Bi}_2}{k}\theta_2, \quad Y=T, \quad 0\le X<L,$$

$$\frac{\partial \theta_2}{\partial Y}=0, \quad Y=0, \quad 0\le X<L, \tag{9}$$

$$\frac{\partial \theta_2}{\partial X}=-\frac{\mathrm{Bi}_2}{k}\theta_2, \quad X=L, \quad 0\le Y\le T.$$

Substitute the boundary conditions of (7) and (9) into the governing equations (6) and (8), the temperature distribution of the fin and the substrate can be solved and obtained as follows:

$$\begin{aligned}\theta_1(X,Y)&=1+b_0\left[1+\mathrm{Bi}_1(W+X)\right]\\&\quad+\sum_{n=1}^{\infty}b_n\frac{\left[\cosh\mu_n(W+X)+\left(\mathrm{Bi}_1/\mu_n\right)\sinh\mu_n(W+X)\right]}{\cosh\mu_nW+\left(\mathrm{Bi}_1/\mu_n\right)\sinh\mu_nW}\\&\quad\times\cos\mu_nY,\end{aligned} \tag{10}$$

$$\begin{aligned}\theta_2(X,Y)&=\frac{\sum_{n=1}^{\infty}a_n\left[\cosh\lambda_m(L-X)+\left(\mathrm{Bi}_2/k\lambda_n\right)\sinh\lambda_n(L-X)\right]}{\cosh\lambda_nL+\left(\mathrm{Bi}_2/k\lambda_n\right)\sinh\lambda_nL}\\&\quad\times\cos\lambda_nY,\end{aligned} \tag{11}$$

where the eigenvalues, respectively, are

$$\mu_n = n\pi, \qquad \lambda_n \tan(\lambda_n T) = \frac{\mathrm{Bi}_2}{k}. \tag{12}$$

One more boundary condition for (8) is

$$\frac{\partial \theta_1}{\partial X} = -\mathrm{Bi}_2 \theta_1, \quad X = 0, \quad T \le Y \le 1. \tag{13}$$

Substitute the boundary condition into (11), and the following equation can be obtained:

$$\mathrm{Bi}_2 + b_0 \left[\mathrm{Bi}_1 + \mathrm{Bi}_2 \left(1 + \mathrm{Bi}_1 W\right)\right] + \sum_{n=1}^{\infty} b_n \left(\mathrm{Bi}_2 + \mu_n \frac{\tanh \mu_n W + \mathrm{Bi}_1/\mu_n}{1 + \mathrm{Bi}_1/\mu_n \tanh \mu_n W}\right) \cos \mu_n Y = 0, \quad T \le Y \le 1. \tag{14}$$

Next, the temperature and the heat transfer of the two regions of the L-shaped domain can be matched along the common boundary. The conditions are given as

$$\theta_1(0, Y) = \theta_2(0, Y), \quad 0 \le Y \le T, \qquad \frac{\partial \theta_1(0, Y)}{\partial X} = k \frac{\partial \theta_1(0, Y)}{\partial X}, \quad 0 \le Y \le T. \tag{15}$$

Substituting the boundary conditions into (10) and (11) yields

$$1 + b_0 \left(1 + \mathrm{Bi}_1 W\right) + \sum_{n=1}^{\infty} b_n \cos \mu_n Y = \sum_{n=1}^{\infty} a_n \cos \lambda_n Y, \quad 0 \le Y \le T, \tag{16}$$

$$-k \sum_{n=1}^{\infty} a_n \left[\lambda_n \frac{\tanh \lambda_n L + \mathrm{Bi}_2/(k\lambda_n)}{1 + (\mathrm{Bi}_2/k\lambda_n) \tanh \lambda_n L}\right] \cos \lambda_n Y = b_0 \mathrm{Bi}_1 + \sum_{n=1}^{\infty} b_n \left(\mu_n \frac{\tanh \mu_n W + \mathrm{Bi}_1/\mu_n}{1 + \mathrm{Bi}_1/\mu_n \tanh \mu_n W}\right) \cos \mu_n Y, \quad 0 \le Y \le T. \tag{17}$$

For calculating the unknown coefficients a_n and b_n, this study will first use the series truncation method and truncation to N terms. The process steps are as follows. Multiplying (17) by $\cos \lambda_m Y$ and then integrating over the range from 0 to T define the relation between the a_n and b_n; namely,

$$a_m = \left(-\frac{b_0 \mathrm{Bi}_1 (\sin \lambda_m T)}{\lambda_m} - \sum_{n=1}^{\infty} b_n \mu_n \frac{\tanh \mu_n W + (\mathrm{Bi}_1/\mu_n)}{1 + (\mathrm{Bi}_1/\mu_n) \tanh \mu_n W} \times \int_0^T \cos \lambda_m Y \cos \mu_n Y \, dY \right) \times \left(\frac{k}{4\lambda_m} \left(2\lambda_m T + \sin 2\lambda_m T\right) \lambda_m \times \frac{\tanh \lambda_m L + \mathrm{Bi}_2/(k\lambda_m)}{1 + (\mathrm{Bi}_2/k\lambda_m) \tanh \lambda_m L} \right)^{-1}, \quad \text{where } m = 1, 2, 3, \ldots. \tag{18}$$

Thus, it remains to determine the coefficients b_n. However, the combined complexity of the governing relations, namely, (14), (16), and (18), precludes the possibility of obtaining an explicit expression for the coefficients b_n. In fact, these coefficients can only be approximately determined. The temperature distributions $\theta_1(X, Y)$ and $\theta_2(X, Y)$ are approximated by the first N terms in each of the series expansions, (10) and (11), respectively, and the relations (14) and (16) are accordingly modified to

$$1 + b_0^* \left(1 + \mathrm{Bi}_1 W\right) + \sum_{n=1}^{N} b_n^* \cos \mu_n Y + \left(\left(\frac{b_0^* \mathrm{Bi}_1 (\sin \lambda_n T)}{\lambda_n} - \sum_{m=1}^{N} b_m^* \mu_m \frac{(\tanh \mu_m W + \mathrm{Bi}_1/\mu_m)}{(1 + (\mathrm{Bi}_1/\mu_m) \tanh \mu_m W)} \times \int_0^T \cos \lambda_n Y \cos \mu_m Y \, dY \right) \times \left(\frac{k}{4\mu_n} \left(2\mu_n T + \sin 2\mu_n T\right) \tanh \lambda_n \right)^{-1} \right) \cos \lambda_n Y = 0, \quad 0 \le Y \le T, \tag{19}$$

$$\mathrm{Bi}_2 + b_0^* \left[\mathrm{Bi}_1 + \mathrm{Bi}_2 \left(1 + \mathrm{Bi}_1 W\right)\right] + \sum_{n=1}^{N} b_n^* \left[\mathrm{Bi}_2 + \frac{\mu_n (\tanh \mu_n W + \mathrm{Bi}_1/\mu_n)}{1 + (\mathrm{Bi}_1/\mu_n) \tanh \mu_n W}\right] \cos \mu_n Y = 0, \quad T \le Y \le 1. \tag{20}$$

Equations (19) and (20) can be further multiplied by $\cos \mu_n$; (19) is integrated over the range $0 \le Y \le$

T and (20) is integrated over the range $T \le Y \le 1$. Then the coefficients b_n^* of N terms can be determined.

Besides, the coefficients a_n^* have been replaced using the approximate form of (18); namely,

$$\begin{aligned} a_m^* = & \left(-\frac{b_0 \mathrm{Bi}_1 (\sin \lambda_m T)}{\lambda_m} \right. \\ & - \sum_{n=1}^{N} b_n^* \mu_n \frac{\tanh \mu_n W + \mathrm{Bi}_1/\mu_m}{1 + (\mathrm{Bi}_1/\mu_m) \tanh \mu_m W} \\ & \left. \times \int_0^T \cos \lambda_m Y \cos \mu_n Y \, dY \right) \\ & \times \left(\frac{k}{4\mu_m} (2\lambda_m T + \sin 2\lambda_m T) \lambda_m \right. \\ & \left. \times \frac{\tanh \lambda_m L + \mathrm{Bi}_2/(k\lambda_m)}{1 + \mathrm{Bi}_2 \tanh \lambda_m L/(k\lambda_m)} \right)^{-1}, \\ & m = 1, 2, 3, \ldots, N. \end{aligned} \tag{21}$$

Next, to compare the results obtained from the series truncation method, the present research uses the point-matching method [13] for calculating the coefficients of a_n^* and b_m^*. Choose N points along the boundary at $X = 0$, and set

$$y_i = \frac{i-1}{N}, \quad \text{where } i = 1, 2, 3, \ldots, N. \tag{22}$$

Truncate b_n^* to N terms and a_m^* to M terms where

$$M = \text{floor function } (NT) + 1. \tag{23}$$

Equations (14), (16), and (17) can be rewritten as the following equations:

$$\begin{aligned} & \mathrm{Bi}_2 + b_0^* \left[\mathrm{Bi}_1 + \mathrm{Bi}_2 (1 + \mathrm{Bi}_1 W) \right] \\ & + \sum_{n=1}^{N} b_n^* \left(\mathrm{Bi}_2 + \mu_n \frac{\tanh \mu_n W + \mathrm{Bi}_1/\mu_n}{1 + \mathrm{Bi}_1/\mu_n \tanh \mu_n W} \right) \cos \mu_n Y_i = 0, \\ & \qquad i = M + 1 \text{ to } N, \\ & 1 + b_0^* (1 + \mathrm{Bi}_1 W) + \sum_{n=1}^{N} b_n^* \cos \mu_n Y_i \\ & = \sum_{m=1}^{M} a_m^* \cos \lambda_m Y_i, \quad i = 1 \text{ to } M, \\ & - k \sum_{m=1}^{M} a_m^* \left[\lambda_m \frac{\tanh \lambda_m L + \mathrm{Bi}_2/(k\lambda_m)}{1 + \mathrm{Bi}_2 \tanh \lambda_m L/(k\lambda_m)} \right] \cos \lambda_m Y_i \\ & = b_0^* \mathrm{Bi}_1 + \sum_{n=1}^{N} b_n^* \left(\mu_n \frac{\tanh \mu_n W + \mathrm{Bi}_1/\mu_n}{1 + \mathrm{Bi}_1/\mu_n \tanh \mu_n W} \right) \cos \mu_n Y_i, \\ & \qquad i = 1 \text{ to } M. \end{aligned} \tag{24}$$

The mean temperature, θ_m, of the entire thermal dissipation substrate and fin can be obtained by the following equation:

$$\begin{aligned} \theta_m = & \frac{1}{W} \int_0^{-W} \int_0^1 \theta_1 (X, Y) \, dY \, dX \\ & + \frac{1}{LT} \int_0^L \int_0^T \theta_2 (X, Y) \, dY \, dX. \end{aligned} \tag{25}$$

The mean temperature can be rewritten in a more detailed form as follows:

$$\begin{aligned} \theta_m = & W + b_0^* \left(W + \frac{W^2 \mathrm{Bi}_1}{2} \right) \\ & + \sum_{n=1}^{N} b_n^* \left(\left(\frac{1}{\mu_n^2} \sinh \mu_n W + \frac{\mathrm{Bi}_1}{\mu_n^3} \cosh \mu_n W - \frac{\mathrm{Bi}_1}{\mu_n^3} \right) \right. \\ & \left. \times \left(\cosh \mu_n W + \frac{\mathrm{Bi}_1}{\mu_n} \sinh \mu_n W \right)^{-1} \right) \sin \mu_n P. \end{aligned} \tag{26}$$

The heat transfer rate for the fin is derived as

$$Q = -\int_0^T \left. \frac{\partial \theta_2}{\partial X} \right|_{X=0} dY. \tag{27}$$

Integrating (27) gives

$$Q = \sum_{m=1}^{N} a_m^* \frac{\tanh \lambda_m L + \mathrm{Bi}_2/k\lambda_m}{1 + (\mathrm{Bi}_2/k\lambda_m) \tanh \lambda_m L} \sin (\lambda_m T). \tag{28}$$

The method of numerical analysis was the Gauss-Seidel method and the program was aided by Visual C^{++}. The coefficients for temperature field in (10) and (11) were evaluated with the aid of (19)-(20) obtained by series truncation method and (24) obtained by point-matching method. And then local dimensionless temperature distributions θ_1 and θ_2 can be obtained. Then mean temperature θ_m and heat transfer rate Q can be obtained in (26) and (28).

3. Results and Discussion

In order to estimate the series convergence, the present research tests the term of the coefficients N. When the term of the coefficients N is set as $N = 60$, the precision of the coefficient converges to five decimal places. Therefore, the present investigation uses $N = 80$ to calculate the results from Figures 4, 5, 6, 7, 8, and 9 in order to ensure convergence. Table 1 shows the coefficient obtained by both the series truncation method and point-matching method and compares the precision by using the two different methods. The result shows that the point-matching method obtained the same degree of precision with the series truncation method, with easier calculation than series truncation method.

Figures 4 and 5 show the isotherms of the substrate and fins obtained by both the series truncation method and point-matching method. As the figures show, under the different parameter conditions and dimensions, the trends

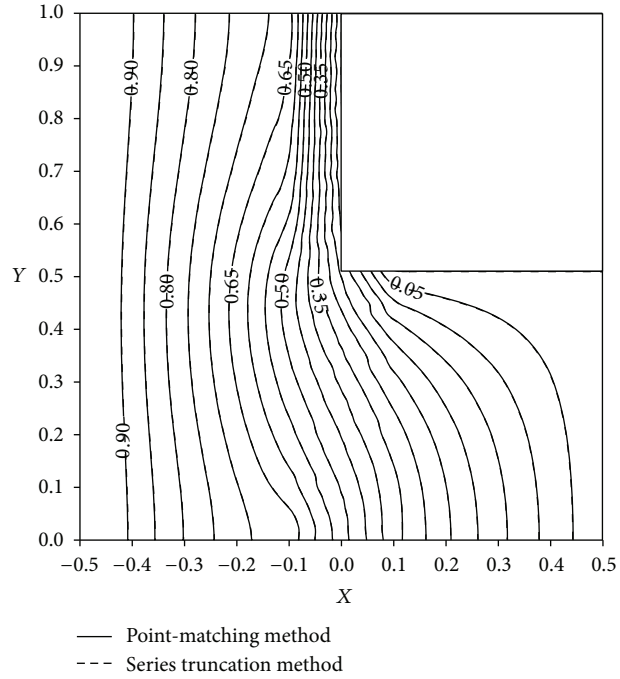

Figure 4: The isotherms for $T = 0.5$, $L = 0.5$, $W = 0.5$, $\mathrm{Bi}_1 = 100$, $\mathrm{Bi}_2 = 1$, and $k = 0.01$.

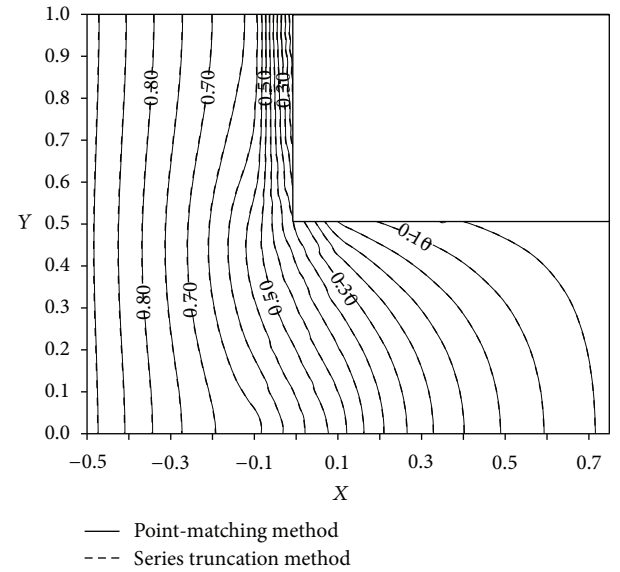

Figure 5: The isotherms for $T = 0.5$, $L = 0.75$, $W = 0.5$, $\mathrm{Bi}_1 = 10$, $\mathrm{Bi}_2 = 1.0$, and $k = 0.1$.

of the isotherm exhibit good agreement obtained by the two different methods. The temperature distribution from the left-hand side of the high temperature of the substrate gradually decreases to the right-hand side of the lower temperature of the fin. Besides, based on the boundary conditions, the isotherms are both symmetric to $Y = 0$ and $Y = 1$.

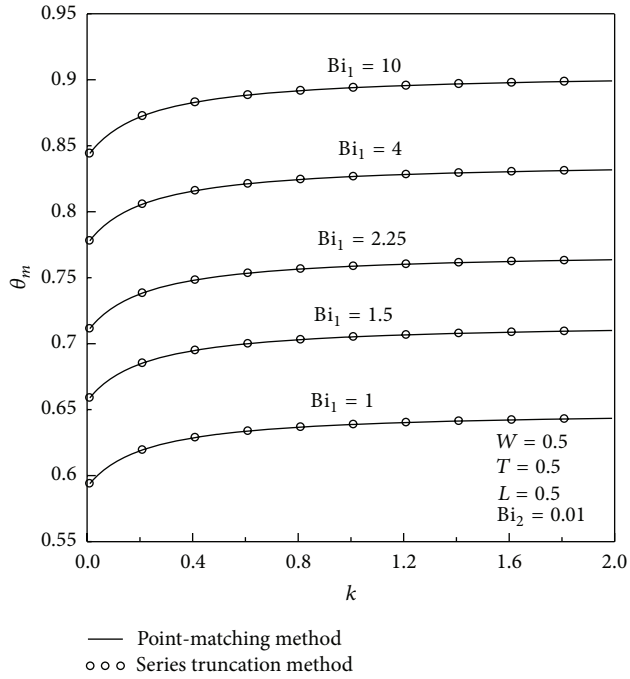

Figure 6: Effects of the thermal conductivities ratio on mean temperature under different Bi_1.

Figure 6 shows the effects of the thermal conductivities ratio ($k = k_2/k_1$) on the mean temperature under different Bi_1. The condition of Bi_2 set in the figure is $\mathrm{Bi}_2 = 0.01$ (where $\mathrm{Bi}_2 = h_{\infty 2}P/k_1$). Owing to the Bi_2 being a small value, 0.01, it is under the setting value of the case, and the value of k_1 is larger than the value of $h_{\infty 2}P$. The ability of conduction heat transfer in the substrate is greater than the ability of convection heat transfer on the fin side. Besides, an increase in the k will bring about a decrease in the k_1 and increase the values of Bi_1 (where $\mathrm{Bi}_1 = h_{\infty 1}P/k_1$). This will lead to the increased values of $h_{\infty 1}$ enhancing the ability of convection heat transfer on the thermal dissipation substrate side and increasing the mean temperature. Besides, since the definition of the Bi_1 is $h_{\infty 1}P/k_1$, the larger value of Bi_1 will lead to an increased heat transfer rate and elevated mean temperature.

Figure 7 shows the effects of the length of the fin on mean temperature under five different values of Bi_2. The mean temperature is defined as (26), when the increased length of the fin L will lead to an increased area of the fins and achieve better heat dissipation; that is, the mean temperature decreases as the length of the fin L increases. Furthermore, since $\mathrm{Bi}_2 = h_{\infty 2}P/k_1$, the larger values of Bi_2 mean better convection heat transfer on the fin side, better heat dissipation, and decreased mean temperature.

Figure 8 shows the effects of the length of the fin L on heat transfer rate Q under five different values of thermal conductivities ratio k. The condition of $L = 0$ means the case without fin and only with the substrate. The smaller values of k mean that the conduction heat transfer of the substrate is larger, leading to an increased heat transfer rate. As the same

Table 1: Estimating the precision of the coefficient under two different methods.

$T = 0.5, L = 0.5, W = 0.5, \mathrm{Bi}_1 = 100, \mathrm{Bi}_2 = 0.01, k = 0.1, N = 80$ Series truncation method/point-matching method		
b_0^* −0.000429/−0.000427	b_1^* −0.0098/−0.00097	b_2^* 0.004091/0.004087
b_3^* 0.004331/0.004326	b_5^* 0.000741/0.000735	b_{10}^* 0.000827/0.000806
b_{20}^* 0.000344/0.000331	b_{30}^* 0.000269/0.000265	b_{40}^* 0.000087/0.000081
b_{50}^* 0.000383/0.0000377	b_{60}^* 0.000093/0.000091	b_{80}^* 0.000003/0.000002
a_1^* −0.00702/−0.00688	a_2^* 0.007064/0.007011	a_3^* 0.000121/0.000113
a_9^* 0.000479/0.000471	a_{12}^* 0.000230/0.000298	a_{13}^* −0.000086/−0.000086
a_{18}^* 0.000041/0.000039	a_{19}^* −0.000027/−0.000026	a_{39}^* −0.000005/−0.000003

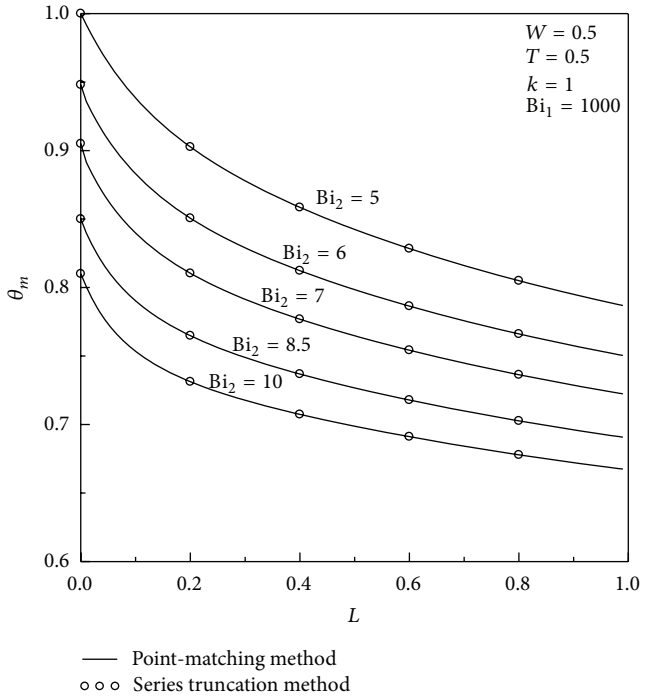

Figure 7: Effects of the length of the fin on mean temperature under different Bi_2.

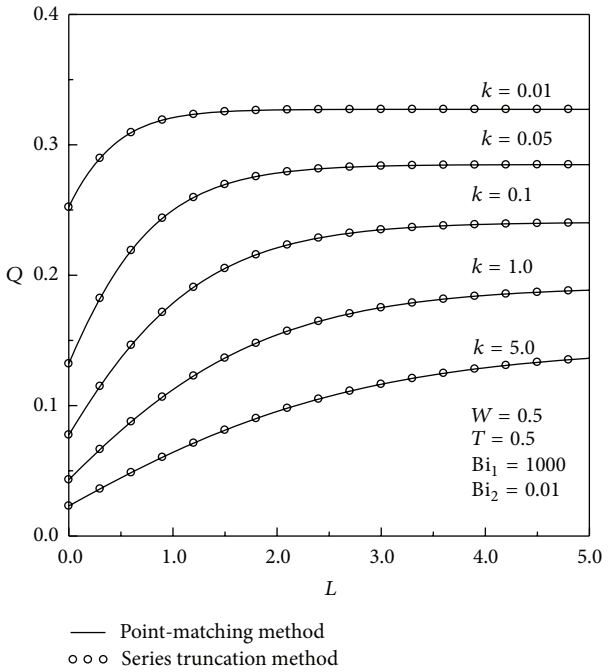

Figure 8: Effects of the length of the fin on heat transfer rate under different thermal conductivity ratios.

situation of $L = 0$, under the range of $1 \le L \le 5$, the smaller values of k increase the Q. Besides, along with the L increase, the Q will increase to a maximum value. Then the increased L will have no influence on the Q (e.g., under $k = 0.01$, the maximum Q is 0.32471); that is, when L reaches the length of finishing heat dissipation, increasing the length of the fin will not influence the heat transfer rate.

Figure 9 shows the effects of the Bi_2 on the heat transfer rate between the interface of thermal dissipation substrate and fins ($X = 0$, $0 \le Y \le T$) under five different values of the height of the fin. Both the horizontal axis and the vertical axis are logarithmic coordinates. As the figure shows, increasing the Bi_2 will lead to an increased heat transfer rate. Furthermore, the larger value of the height of the interface between substrate and the fin will increase the heat transfer area, leading to an increased heat transfer rate.

Figure 10 shows the effects of the length of the fin L on fin performance under five different values of thermal conductivities ratio k, where the Q_s are defined as dimensionless heat transfer rate without fins and only with the substrate. As the figure shows, under the case of $L = 0$, the Q/Q_s are all 1.0. Under the range of $0 < L \le 5$, the smaller values of k increase the fin performances. Besides, along with the L increase, the fin performances will increase to a maximum value. Then the increased L will have no influence on the fin performances; that is, when L reaches the length of finishing heat dissipation, increasing the length of the fin will not influence the fin performances.

4. Conclusions

The following conclusions can be drawn from the results of the present theoretical study.

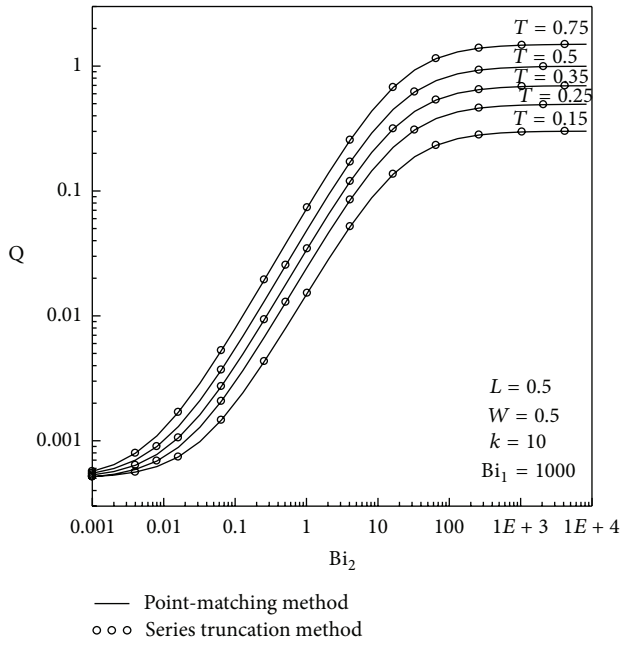

Figure 9: Effects of the Bi_2 on heat transfer rate under different heights of the fin.

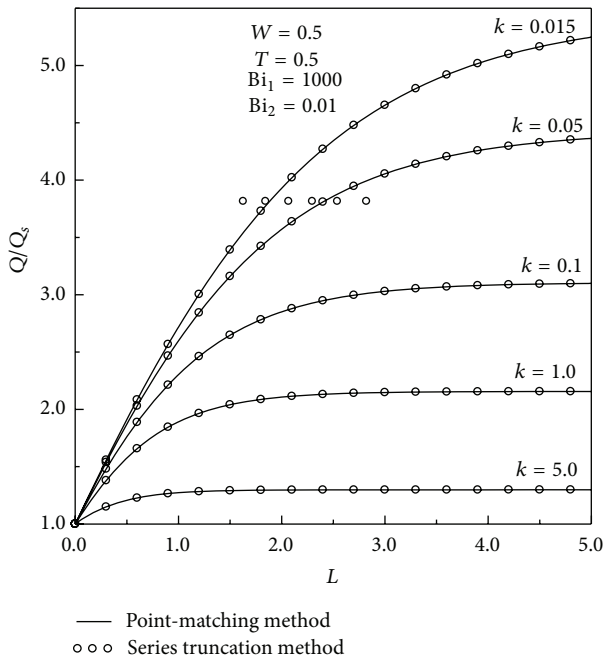

Figure 10: Effects of the length of the fin on fin performances under different thermal conductivity ratios.

(1) The results show that the point-matching method obtained the same degree of precision as that of the series truncation method. However, the point-matching method is more easily calculated than the series truncation method.

(2) An increase in thermal conductivities ratio, k, will increase the ability of convection heat transfer of the substrate side and increase the mean temperature. Besides, the larger value of Bi_1 will lead to an increased heat transfer rate as well as an increased mean temperature.

(3) The mean temperature decreases as the length of the fin L increases. Furthermore, the larger values of Bi_2 will bring about better heat dissipation and decrease the mean temperature.

(4) The smaller values of k will increase heat transfer rate. Besides, the L increase will also increase the heat transfer rate to a maximum value. Then increasing the L will no longer influence the heat transfer rate.

(5) The increased Bi_2 will lead to an increased heat transfer rate, Q. Furthermore, the larger value of the height of the interface between substrate and the fin will increase the heat transfer area and lead to an increased heat transfer rate.

Nomenclature

Bi_1: Biot number, $h_{\infty 1}P/k_1$
Bi_2: Biot number, $h_{\infty 2}P/k_1$
$h_{\infty 1}$, $h_{\infty 2}$: Convection heat transfer (W/m^2·K)
k_1, k_2: Thermal conductivities (W/m·K)
k: Thermal conductivities ratio, k_2/k_1
l: Fin length (m)
L: Dimensionless fin length, l/p
P: Half fin pitch (m)
t: Half fin-base height (m)
T: Dimensionless half fin-base height, t/p
w: Thermal dissipation substrate width (m)
W: Dimensionless width of the substrate, w/p
x: Horizontal axis (m)
X: Dimensionless horizontal axis, x/p
y: Vertical axis (m)
Y: Dimensionless vertical axis, y/p
T_1: Temperature distribution of thermal dissipation substrate (K)
T_2: Temperature distribution of fin (K)
θ_1: Dimensionless temperature distribution of substrate $(T_1(x, y) - T_{\infty 2})/(T_{\infty 1} - T_{\infty 2})$
θ_2: Dimensionless temperature distribution of fin $\theta_2 = (T_2(x, y) - T_{\infty 2})/(T_{\infty 1} - T_{\infty 2})$.

Subscripts

$\infty 1$: Thermal dissipation substrate side
$\infty 2$: Fin side
1: Thermal dissipation substrate
2: Fin.

Conflict of Interests

The author declares that there is no conflict of interests regarding the publication of this paper.

Acknowledgment

The author gratefully acknowledges the support provided to this project by the Ministry of Science and Technology of Taiwan under Contracts nos. NSC-101-2221-E-019-044 and MOST-103-2221-E-019-061.

References

[1] M. Levitsky, "The criterion for validity of the fin approximation," *International Journal of Heat and Mass Transfer*, vol. 15, no. 10, pp. 1960–1963, 1972.

[2] R. K. Irey, "Errors in the one-dimensional fin solution," *ASME, Journal of Heat Transfer*, vol. 90, pp. 175–176, 1968.

[3] W. Lau and C. W. Tan, "Errors in one-dimensional heat transfer analysis in straight and annular fins," *Journal of Heat Transfer*, vol. 95, no. 4, pp. 549–551, 1973.

[4] E. M. Sparrow and L. Lee, "Effects of fin base-temperature depression in a multifin array," *Journal of Heat Transfer*, vol. 97, no. 3, pp. 463–465, 1975.

[5] N. V. Suryanarayana, "Two-dimensional effects on heat transfer rates from an array of straight fins," *Journal of Heat Transfer*, vol. 99, no. 1, pp. 129–132, 1977.

[6] P. J. Heggs and P. R. Stones, "The effects of dimensions on the heat flowrate through extended surfaces," *Journal of Heat Transfer*, vol. 102, no. 1, pp. 180–182, 1980.

[7] P. J. Heggs, D. B. Ingham, and M. Manzoor, "The analysis of fin assembly heat transfer be a series truncation method," *Journal of Heat Transfer*, vol. 104, no. 1, pp. 210–212, 1982.

[8] M. Manzoor, D. B. Ingham, and P. J. Heggs, "The accuracy of perfect contact fin analyses," *Journal of Heat Transfer*, vol. 106, no. 1, pp. 234–237, 1984.

[9] A. S. Wood, G. E. Tupholme, M. I. H. Bhatti, and P. J. Heggs, "Performance indicators for steady-state heat transfer through fin assemblies," *Journal of Heat Transfer*, vol. 118, no. 2, pp. 310–316, 1996.

[10] C.-C. Wang, L.-P. Chao, and W.-J. Liao, "Hybrid spline difference method (HSDM) for transient heat conduction," *Numerical Heat Transfer, Part B: Fundamentals*, vol. 61, no. 2, pp. 129–146, 2012.

[11] C.-C. Wang, J.-H. Huang, and D.-J. Yang, "Cubic spline difference method for heat conduction," *International Communications in Heat and Mass Transfer*, vol. 39, no. 2, pp. 224–230, 2012.

[12] F. Mabood, W. A. Khan, and A. I. M. Ismail, "Series solution for steady heat transfer in a heat-generating fin with convection and radiation," *Mathematical Problems in Engineering*, vol. 2013, Article ID 806873, 7 pages, 2013.

[13] H.-P. Hu and R.-H. Yeh, "Theoretical study of the laminar flow in a channel with moving bars," *Journal of Fluids Engineering*, vol. 131, no. 11, Article ID 111102, 7 pages, 2009.